Available online at www.sciencedirect.com

ScienceDirect

Procedia Structural Integrity 53 (2024) 81–88

Structural Integrity Procedia

www.elsevier.com/locate/procedia

Third European Conference on the Structural Integrity of Additively Manufactures Materials (ESIAM23)

Evaluation of the structural strength of anisotropic PLA components manufactured by 3D printing

Armando Ramalho[a,b,*], Dino Freitas[c,d,e], Henrique Almeida[c,f]

[a] *Polytechnic Institute of Castelo Branco, 6000-767, Castelo Branco, Portugal*
[b] *CEMMPRE, University of Coimbra, 3030-790, Coimbra, Portugal*
[c] *School of Technology and Management, Polytechnic Institute of Leiria, 2411-901, Leiria, Portugal*
[d] *ciTechCare, Polytechnic Institute of Leiria, 2411-901, Leiria, Portugal*
[e] *aTOPlab, Polytechnic Institute of Leiria, 2411-901, Leiria, Portugal*
[f] *CIIC, Polytechnic Institute of Leiria, 2411-901, Leiria, Portugal*

Abstract

Predicting the mechanical strength of components manufactured by additive processes is a challenging task that is difficulted by the complexity of the geometries fabricated by these processes, along with the anisotropy enhanced by the layer-by-layer manufacturing method and the difficulty in quickly obtaining the elastic and strength properties of the materials, which are strongly influenced by the manufacturing parameters. The use of 3D CAD models in the design phase of components manufactured by 3D printing facilitates the use of the finite element method in assessing their strength and simulating their in-service behavior. However, the finite element analysis of 3D printed parts using anisotropic material behaviour are rare and restricted to simple geometries. To deal with the anisotropy of materials, intense research has been carried out for the last decades in the field of evaluating the mechanical strength of composite materials, introducing several specific failure criteria.
In this article, the in-service behaviour of PLA components manufactured by 3D printing is simulated, applying criteria usually used in the study of composite materials to evaluate their mechanical strength. The simulation through the finite element method was developed on the Hexagon Marc/Mentat software, using the Maximum Stress and Hoffman failure criteria.

© 2023 The Authors. Published by Elsevier B.V.
This is an open access article under the CC BY-NC-ND license (https://creativecommons.org/licenses/by-nc-nd/4.0)
Peer-review under responsibility of the scientific committee of the ESIAM23 chairpersons

Keywords: Additive manufacturing; Anisotropic materials; Failure criteria; Mechanical strength

* Corresponding author. Tel.: +351-272-339-600.
E-mail address: aramalho@ipcb.pt

2452-3216 © 2023 The Authors. Published by ELSEVIER B.V.
This is an open access article under the CC BY-NC-ND license (https://creativecommons.org/licenses/by-nc-nd/4.0)
Peer-review under responsibility of the scientific committee of the ESIAM23 chairpersons
10.1016/j.prostr.2024.01.011

1. Introduction

Additive manufacturing was initially used to manufacture prototypes, being now increasingly used to manufacture final products. Its ability to produce small series of components with complex geometries and low material waste has favoured its rapid growth, with applications in the most diverse fields, from aeronautics to the automotive industry and to medicine (Khosravani *et al* 2022) (Shu *et al* 2021).

The use of Fused Filament Fabrication (FFF) in progressively demanding situations regarding structural requirements demands increasingly reliable designs. In this manufacturing process, more tough, rigid and tenacious materials are more and more used, such as Polylactic Acid (PLA), Acrylonitrile Butadiene Styrene (ABS), Polyethene Terephthalate Glycol (PETG), or polyamides, often with the filaments incorporating short fibres, with the aim of improving their mechanical behaviour.

The layered manufacturing method associated with the FFF process is prone to introducing anisotropy into the materials thus obtained, specifically orthotropy (Song *et al* 2017) (Vukasovic *et al* 2019) (Grant *et al* 2021).

The design of products with complex geometries is increasingly dependent on the development of numerical models using the finite element method, which allow the simulation of the mechanical in-service behaviour of these components. There are several studies in which the finite element method is used to characterize the mechanical behaviour of components manufactured by 3D printing, in which the materials are considered isotropic (Abueidda *et al* 2019) (Shu *et al* 2021). Studies in which numerical finite element models use anisotropic behaviour of materials are usually applied to simple geometries and are uncommon (Zouaoui *et al* 2019) (Torre and Brischetto 2022).

The authors in (Ramalho *et al* 2023) presented a preliminary work, in which a numerical finite element model was developed to characterize the in-service behaviour of the bushing of the support of a tilting drawer, manufactured in PLA using the FFF process. In this study it was considered that PLA had an orthotropic behaviour, the mechanical properties were obtained from literature (Song *et al* 2017), and the structural integrity of the bushing was evaluated by comparing the normal stresses in the anisotropy directions with the respective yield stresses.

To deal with the anisotropy of materials and the presence of several phases, intense research has been carried out for the last decades in the field of evaluating the mechanical strength of composite materials, introducing several specific failure criteria (Hinton *et al* 2004) (Camanho 2002) (De Luca and Caputo 2017).

Some authors have suggested the use of composite material failure criteria to evaluate the structural integrity of products manufactured by 3D printing (Ahn and Baek 2003) (Khosravani *et al* 2022) (Yao *et al* 2020).

In this article, the in-service behaviour of PLA components manufactured by 3D printing is simulated, applying criteria usually used in the study of composite materials to evaluate their mechanical strength. The previous numerical finite element model developed by the authors (Ramalho *et al* 2023) was updated and implemented on the Hexagon Marc/Mentat software to evaluate the structural integrity of a bushing made with PLA orthotropic material, using the Maximum Stress and Hoffman failure criteria.

2. Methodology

2.1. The designed component

The component analysed in this study is a bushing of an hinged drawer support, that was broken. The drawer and its content have a design weight of 20 kgf. The parts of the hinged drawer support were made in ABS and manufactured by injection. A preliminary reverse engineering bushing design was done in a previous work (Ramalho *et al* 2023):

- The bushing and the corresponding tightening screw were designed in the Solidworks 2022 software;
- The screw-tightening torque was experimentally obtained using a torque wrench;
- The loading on the bushing corresponds to the design weight supported by the drawer and was assumed to be applied to half of its outer surface;

- The pre-manufacturing process of the bushing part was performed on the Ultimaker Cura 5.1.0 software;

- The Ultimaker S5 Printer with the following manufacturing parameters was used: the bushing was printed in PLA material in the XY plane, using the fine quality profile, a 0.4 mm AA print core, 100% infill, 0.15 mm layer height, two wall line counts with 0.4 mm of thickness, a 210°C nozzle temperature, a build plate temperature of 85°C, a print speed of 45.0 mm/s, supports were used for the fixing top of the bushing, a concentric infill pattern and a top/bottom concentric pattern were used to assure the axisymmetric manufacturing of the bushing.

2.2. Finite element model

All the numerical simulations were performed in a computer running Windows 10, with an Intel(R) Core(TM) i7 processor and 16 GB RAM, using a numerical model developed in the finite element software Hexagon Marc/Mentat 2021.

The previous preliminary finite element model developed by the authors (Ramalho *et al* 2023) is updated and implemented in the Hexagon Marc/Mentat software:

- The tightening, with a steel screw, of the PLA bushing is done through its taper against an ABS support as shown in Fig. 1.

- In the conical tightening is considered a 0.15 friction coefficient between the PLA bushing and the support (Yilmaz 2021).

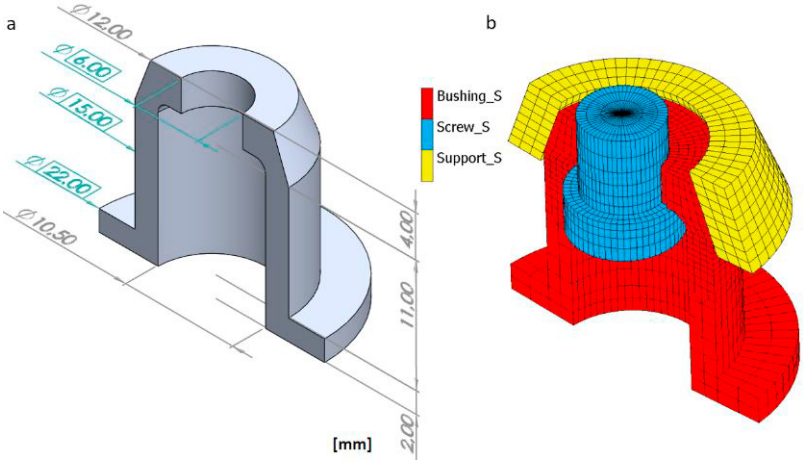

Fig. 1. (a) Geometrical model of half the bushing; (b) cutting of the mesh of the finite element model.

The materials of the screw and the support were assumed to have isotropic behaviour: for the steel was used the Young's modulus E = 200 GPa and the Poison's ratio ν= 0.3; for the ABS was used E = 3200 MPa and ν= 0.43. In contact between the screw and the bushing a 0.49 friction coefficient is assumed.

In the bushing, the anisotropy axis takes into account the pattern of the filling used in the printing process. In this case a concentric pattern was used. In other to consider the variations of the directions of the anisotropy, even in more complex geometries, the local element axis are considered as the anisotropy axis. For these cases it is important to use a structured mesh. In this case an axisymmetric structured mesh was used and the local element axis, used as directions of anisotropy, are presented in Fig. 2.

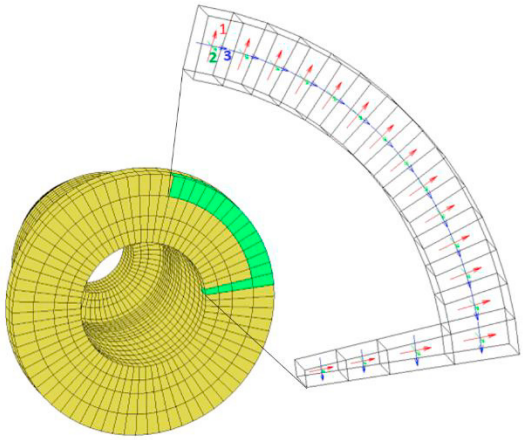

Fig. 2. Detail of the structured axisymmetric mesh with the anisotropy axis.

The imported 3D geometry of the analysed system is meshed in MSC Mentat using 6020 hexahedral full integration linear elements, Hex8, for the bushing, 1680 Hex8 elements for the support and for the screw 1680 Hex8 and 600 pentahedral full integration linear elements, Penta6, were used.

Were considered the following boundary conditions: Boundary condition: the displacements were restricted at the outer surface of the support; the transverse displacement was restricted at the end section of the screw; and contact conditions were considered between the bushing and the screw and the bushing and the support – an algorithm of segment-to-segment contact was adopted.

For the friction it was considered the Coulomb's bilinear friction model.

The loading was applied in two steps: an initial clamp load of 20 N, was applied in the axial direction at the end section of the screw; followed by a vertical load of 100 N that actuates in the 3rd direction at the outer surface of the bushing, through a RBE2 type link.

The boundary conditions and the loading are presented in Fig. 3.

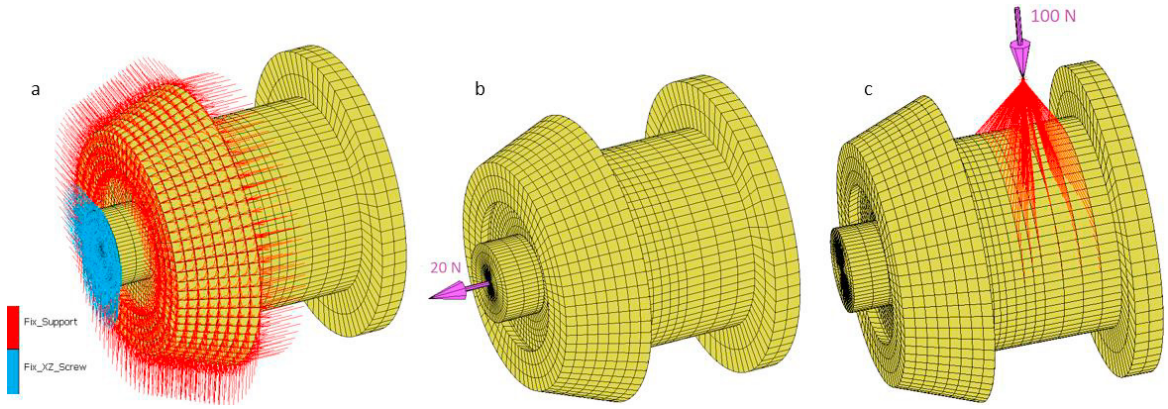

Fig. 3. (a) Displacement boundary conditions; (b) pre-loading – step 1; (c) loading – step 2.

The material behaviour is intrinsically related with the pattern of the filling and the staking used in the manufacturing process. Therefore, it is important to take these settings into account in the slicing software.

Attending to the adopted parameters in the pre-manufacturing process of the bushing, performed on the Ultimaker Cura 5.1.0 software for the Ultimaker S5 printer, an elastic and 3D orthotropic behaviour for the extruded PLA was assumed, with the mechanical properties represented in Table 1, obtained from literature (Song *et al*

2017). The assumed directions for the mechanical characterization are the ones presented in Fig. 2: the directions 1 and 3 are on the construction layer, the 3 in the deposition direction and the 1 in the transverse one; the 2nd direction is in the stacking direction. X_t and X_c are the normal yield stresses in the 1st direction, in tension and compression respectively; Y_t and Y_c are the normal yield stresses in the 2nd direction, in tension and compression respectively; Z_t and Z_c are the normal yield stresses in the 3rd direction, in tension and compression respectively.

Table 1. Mechanical properties of extruded PLA (Song *et al* 2017).

Young's Moduli [MPa]	Normal Tensile Yield Stresses [MPa]	Normal Compressive Yield Stresses [MPa]	Poisson's Ratios	Shear Moduli [MPa]	Shear Yield Strength [MPa]
E_{11}= 4040	X_t = 45.16	X_c = 94.87	ν_{12}=0.37	G_{12} = 1470	S_{12} = 30
E_{22}= 4040	Y_t = 45.16	Y_c = 94.87	ν_{32}=0.34	G_{32} = 1500	S_{32} = 28
E_{33}= 3980	Z_t = 54.84	Z_c = 95.79	ν_{31}=0.34	G_{31} = 1500	S_{31} = 28

2.3. Failure criteria for orthotropic materials

In order to account for the anisotropy in the failure of the bushing, theories from the composite materials were used. Each layer of the manufacturing process is treated as a lamina, and it is assumed that the adopted stacking of these layers forms an orthotropic material.

The mechanical properties for the extruded PLA presented in Table 1 reveals an ultimate tensile strain below 4.5% and a compressive strength substantially superior to the tensile one. Considering these mechanical characteristics and nomenclature, two failure criteria were considered in this study: the Maximum Stress and the Hoffman.

The Maximum Stress Criterion, considers that the material fails when the stress exceeds its admissible value. For this criterion, six failure indexes (FI) are defined, each one related to one condition of failure (Marc® 2021.4), as represented in equation (1).

$$FI\ 1 = \begin{cases} \frac{\sigma_1}{X_t} & if\ \sigma_1 \geq 0 \\ -\frac{\sigma_1}{X_c} & if\ \sigma_1 < 0 \end{cases};\quad FI\ 2 = \begin{cases} \frac{\sigma_2}{Y_t} & if\ \sigma_2 \geq 0 \\ -\frac{\sigma_2}{Y_c} & if\ \sigma_2 < 0 \end{cases};\quad FI\ 3 = \begin{cases} \frac{\sigma_3}{Z_t} & if\ \sigma_3 \geq 0 \\ -\frac{\sigma_3}{Z_c} & if\ \sigma_3 < 0 \end{cases}$$

$$FI\ 4 = \frac{\sigma_{12}}{S_{12}};\quad FI\ 5 = \frac{\sigma_{23}}{S_{23}};\quad FI\ 6 = \frac{\sigma_{31}}{S_{31}} \tag{1}$$

The Hoffman Criterion, considers that the orthotropic material fails when the modulus of the failure index exceeds 1, and allow unequal maximum stresses in tension and compression. At each integration point the failure index is computed by the equation (2), (Marc® 2021.4).

$$FI = [C_1(\sigma_2 - \sigma_3)^2 + C_2(\sigma_3 - \sigma_1)^2 + C_3(\sigma_1 - \sigma_2)^2 + C_4\sigma_1 + C_5\sigma_2 + C_6\sigma_3 + C_7\sigma_{23}^2 + C_8\sigma_{13}^2 + C_9\sigma_{12}^2]$$

$$Were:$$

$$C_1 = \frac{1}{2}\left(\frac{1}{Z_tZ_c} + \frac{1}{Y_tY_c} - \frac{1}{X_tX_c}\right);\ C_2 = \frac{1}{2}\left(\frac{1}{X_tX_c} + \frac{1}{Z_tZ_c} - \frac{1}{Y_tY_c}\right);\ C_3 = \frac{1}{2}\left(\frac{1}{X_tX_c} + \frac{1}{Y_tY_c} - \frac{1}{Z_tZ_c}\right)$$

$$C_4 = \frac{1}{X_t} - \frac{1}{X_c};\ C_5 = \frac{1}{Y_t} - \frac{1}{Y_c};\ C_6 = \frac{1}{Z_t} - \frac{1}{Z_c};\ C_7 = \frac{1}{S_{23}^2};\ C_8 = \frac{1}{S_{13}^2};\ C_9 = \frac{1}{S_{12}^2} \tag{2}$$

3. Results and discussion

In Fig. 4 are represented the Failure Indexes obtained for the Maximum Stress Criterion.

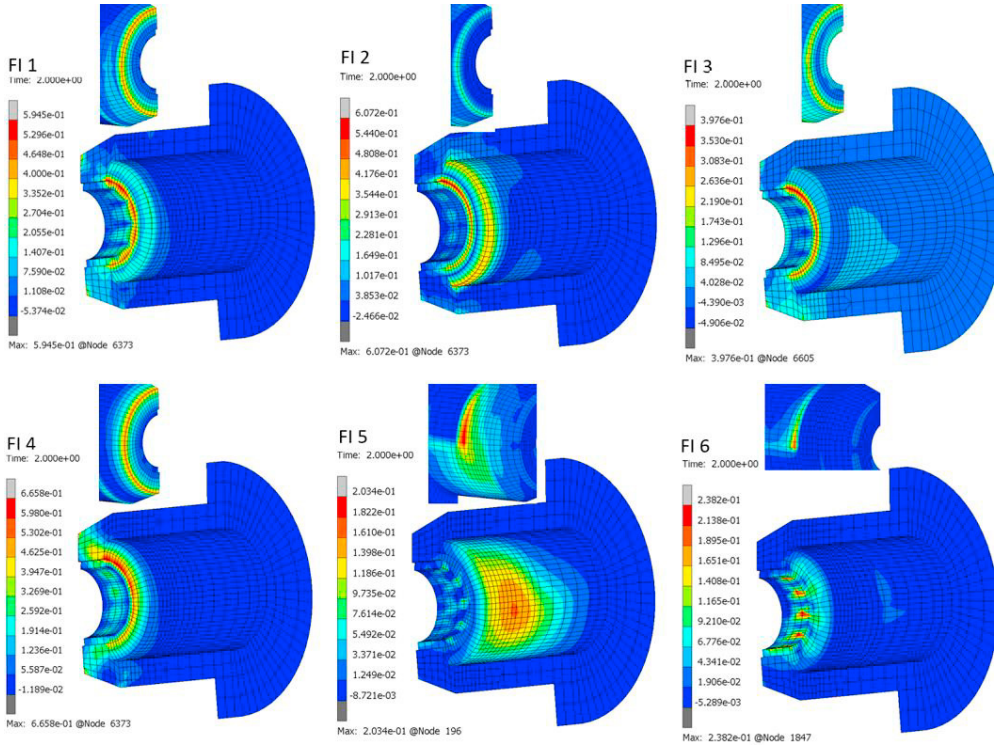

Fig. 4. Failure Indexes obtained the Maximum Stress Criterion.

From the analysis of these results, it appears that all indexes have a value lower than 1, whereby, all the stresses are below the maximum admissible values. So, from this criterion it is possible to assure the structural integrity of the 3D printed bushing , under the in-service loading.

The more critical Failure Index is the fourth (FI 4) and occurs at the interface between the screw head and the bushing. The FI 4 is related to the shear stresses occurring in the 1-2 plane that refers to the axial-radial directions, as shown in Fig. 3.

In Fig. 5 is represented the Failure Index obtained for the Hoffman Criterion.

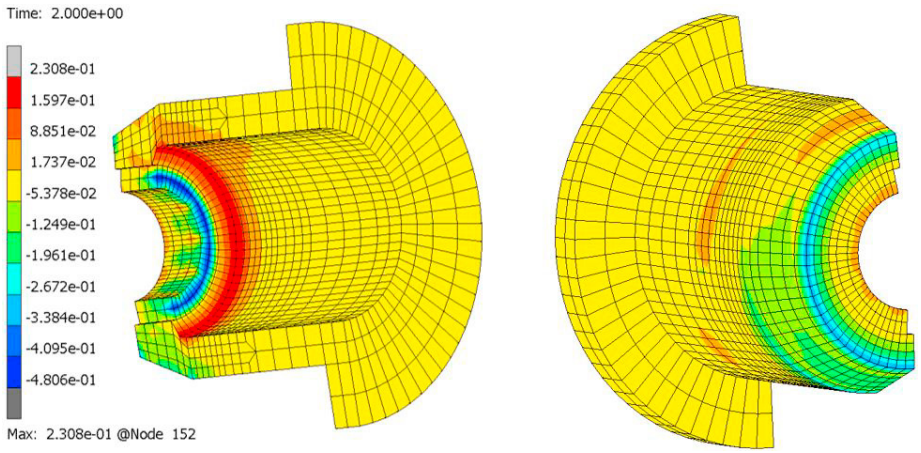

Fig. 5. Failure Indexes obtained the Hoffman Criterion.

From the analysis of these results, it appears that the modulus of Hoffman Failure Index is lower than 1. So, from this criterion it is possible to assure the structural integrity of the 3D printed bushing , under the in-service loading.

It is clear that the maximum modulus of the Hoffman Failure Index occurs at the same position of the maximum value of the fourth Failure Index of the Maximum Stress one. However, the Hoffman Failure Index presents lower values.

From the presented results for both criteria it can be inferred that the structural safety of the bushing can be increased by decreasing the pre-tightening of the screw. To test this hypothesis, a simulation was carried out with a preload of 10 N applied to the screw. In Fig. 6 are presented the Hoffman Failure Index obtained for this simulation. In the simulation it was also verified that there was no significant slippage in the conical clamping. From the presented results the hypothesis was validated.

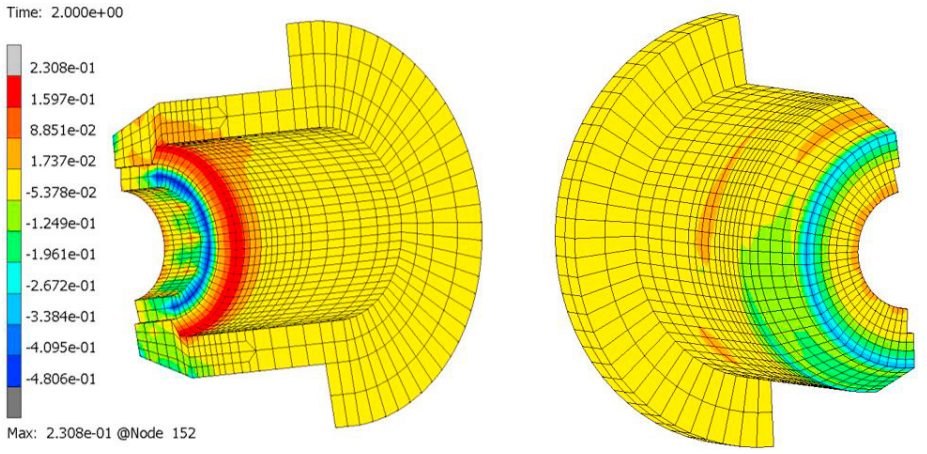

Fig. 6. Failure Indexes obtained from the Hoffman Criterion with half of preload (10 N) applied to the screw.

4. Conclusions

Through this study, it was possible to manufacture by 3D Printing, namely extrusion based additive manufacturing, a bushing that resists to the in-service loading conditions. This study also combined the use of numerical simulation to improve the design of the designated part.

The usefulness of numerical finite element method with the failure criteria extensively used on composite materials in the structural design of parts manufactured by 3D Printing was demonstrated.

The adaptation of the finite numerical models has validated the design phase and can improve the design capabilities of additive manufactured parts. The presented methodology is effective to demonstrate the reliable design of components manufactured by 3D printing.

Acknowledgements

This research is sponsored by national funds through FCT – Fundação para a Ciência e Tecnologia, Portugal under the project UIDB/00285/2020.

References

Abueidda, D.W., Elhebeary, M., Shiang, C.-S. A., Pang, S., Al-Rub, R.K.A., Jasiuk, I.M., 2019. Mechanical properties of 3D printed polymeric Gyroid cellular structures: Experimental and finite element study. Materials and Design 165: 107597.

Ahn, S.H., Baek, C., 2003. Anisotropic Tensile Failure Model of Rapid Prototyping Parts - Fused Deposition Modeling (FDM). International Journal of Modern Physics B, Vol. 17, Nos. 8 & 9: 1510-1516.

Camanho, P.P., 2002. Failure Criteria for Fibre-Reinforced Polymer Composites. DEMEGI, Porto. https://web.fe.up.pt/~stpinho/teaching/feup/y0506/fcriteria.pdf

De Luca, A., Caputo, F., 2017. A review on analytical failure criteria for composite materials. AIMS Materials Science, 4 (5): 1165-1185.

Grant, A., Regez, B., Kocak, S., Huber, J.D., Mooers, A., 2021. Anisotropic properties of 3-D printed Poly Lactic Acid (PLA) and Acrylonitrile Butadiene Styrene (ABS) plastics. Results in Materials, 12: 100227.

Hinton, M.J., Kaddour, A.S., Soden, P.D., 2004. Failure Criteria in Fibre-Reinforced-Polymer Composite: The World-Wide Failure Exercise. Elsevier Science, ISBN 978-0-08-044475-8.

Khosravani, M.R., Berto, F., Majid R. Ayatollahi, M.R., Reinicke, T., 2022. Characterization of 3D-printed PLA parts with different raster orientations and printing speeds. Scientific Reports, 12: 1016, https://doi.org/10.1038/s41598-022-05005-4.

Marc® 2021.4. Volume A: Theory and User Information. Version K7, MARC Analysis Research Corporation. 2021 Hexagon AB.

Ramalho, A., Freitas, D., Almeida, H., 2023. The anisotropy and friction effect in the design of 3D printed PLA parts – A case study. Materials Today: Proceedings. https://doi.org/10.1016/j.matpr.2023.08.196.

Shu, J., Luo, H., Zhang, Y., Liu, Z., 2021. 3D Printing Experimental Validation of the Finite Element Analysis of the Maxillofacial Model. Front. Bioeng. Biotechnol. 9: 694140. doi: 10.3389/fbioe.2021.694140.

Song, Y., Li, Y., Song, W., Yee, K., Lee, K.-Y., Tagarielli, V.L., 2017. Measurements of the mechanical response of unidirectional 3D-printed PLA. Materials and Design, 123: 154-164.

Torre, R., Brischetto, S., 2022. Experimental characterization and finite element validation of orthotropic 3D-printed polymeric parts. International Journal of Mechanical Sciences, 219: 107095.

Vukasovic, T., Vivanco, J.F., Celentano, D., García-Herrera, C., 2019. Characterization of the mechanical response of thermoplastic parts fabricated with 3D printing. Int J Adv Manuf Technol 104: 4207–4218.

Yao, T., Ye, J., Deng, Z., Zhang, K., Ma, Y., Ouyang, H., 2020. Tensile failure strength and separation angle of FDM 3D printing PLA material: Experimental and theoretical analyses. Composites Part B: Engineering, 188: 107894.

Yilmaz, S., 2021. Comparative Investigation of Mechanical, Tribological and Thermo-Mechanical Properties of Commonly Used 3D Printing Materials. European Journal of Science and Technology. Special Issue 32: 827-831.

Zhao, Y., Chen, Y., Zhou, Y., 2019. Novel mechanical models of tensile strength and elastic property of FDM AM PLA materials: Experimental and theoretical analyses. Materials and Design, 181: 108089.

Zouaoui, M., Labergere, C., Gardan, J., Makke, A., Recho, N., Lafon, P., 2019. Finite element modeling and anisotropy implementation in 3D printed structures using an optimized method. 24th French Congress of Mechanics, Brest, on August 26-30, France.